

The Sample Complexity of Differential Analysis for Networks that Obey Conservation Laws

Jiajun Cheng, Anirudh Rayas, Rajasekhar Anguluri, and Gautam Dasarathy

Department of Electrical, Computer, & Energy Engineering, Arizona State University

November 25, 2024

Abstract

1 Introduction

Networks that obey conservation laws maintain balanced flows, ensuring that no flow is generated or lost within the network. The interpretation of flow can vary depending on the specific application. For instance, in electrical circuits, flows might represent the movement of electrical current; in hydraulic networks, they could represent the flow of water; and in social networks, they may reflect a consensus of views in social science. Network systems in many practical applications are not static; their structure evolves over time due to dynamic interactions. Thus, it is crucial to understand these shifts in analysis. Given the importance of understanding how network structures evolve under conservation laws, we want to estimate the *difference matrix* $\Delta^* = B_2^* - B_1^*$ between the structures of two networks that obey conservation laws, where B_1^* and B_2^* are invertible Laplacian matrix represent the structure of the networks given potential data from both. Rayas et al. [1] propose an ℓ_∞ -regularized convex estimator that directly identifies sparse edge changes based on node potential data. Additionally, they establish the convexity of the estimator and demonstrate its superior performance in experiments. In this paper, we mainly focus on the statistical guarantees of this estimator. Building on the *primal-dual witness* framework from [2], we quantify the sample requirement necessary for accurately recovering the true sparse network changes. Specifically, we guarantee that an element-wise ℓ_∞ error bound of order $\mathcal{O}(\sqrt{\frac{p \log(p)}{n}})$ holds with high probability, with a sample complexity satisfying $\Omega(pd^2 \log(p))$, where d represents the maximum degree of any row or column in Δ^* . Finally, we note a gap between our theorem and the results obtained in the experiments. The challenge arise from the *square root perturbation bounds*, which we discuss later in the paper. Addressing this issue could lead to more accurate statistical guarantees.

1.1 Related Work

In many real-world applications, learning the unknown structure of a network is essential for understanding and managing complex systems. This task often involves inferring the structure of graphical models based on node potentials, a topic that has garnered considerable attention in recent years (see, for instance, [3, 4, 5]). Notably, the dynamic nature of networks highlights the importance of studying their evolution over time. The problem of *differential network analysis* has become crucial for several tasks across a wide range of fields, including biomedicine, social networks, and cyber-physical systems [6, 7, 8, 9]. A straightforward approach to identifying sparse changes might involve estimating the structure of each network independently and then comparing them to find differences. However, such a method has a significant drawback: it estimates

parameters unrelated to the specific task, such as edges that remain unchanged over time. In [8], the authors proposed a loss function called the D-trace loss function, which allows direct estimation of the precision matrix difference without attempting to estimate the precision matrices themselves. This loss function can be considered a generalization of the one proposed in [10].

2 Preliminaries and Background

Let a graph $\mathcal{G} = ([p], E)$ be an undirected connected graph, and let $X \in \mathbb{R}^p$ be a p -dimensional vector of *injected flows* at the vertices $[p]$. Let $Y \in \mathbb{R}^p$ be the vector of the *vertex potentials*. The flows and potentials are said to satisfy a *conservation law* with respect to the graph \mathcal{G} if they obey the relationship $Y = (B^*)^{-1}X$, where B^* is an invertible Laplacian matrix associated with \mathcal{G} . That is, at each vertex, the flows directly counteract the injections, and such an equation is called a *balance equation* between potentials and injected flows.

The differential network analysis problem we consider is stated as follows. Consider two networked systems \mathcal{G}_1 and \mathcal{G}_2 with the same node sets but different edge sets. Let $X_1 \sim \mathcal{N}(0, \Sigma_{X_1})$ and $X_2 \sim \mathcal{N}(0, \Sigma_{X_2})$ be the injection vectors at the nodes of \mathcal{G}_1 and \mathcal{G}_2 . Then, the corresponding node potentials $Y_i = (B_i^*)^{-1}X_i$ satisfy $Y_i \sim \mathcal{N}(0, \Theta_i^{*-1})$, where $\Theta_i^* = B_i^* \Sigma_{X_i}^{-1} B_i^*$ and $i \in \{1, 2\}$. We are interested in the difference between the two network structures. Formally, given node potential observations Y_i , estimate $\Delta^* = B_1^* - B_2^*$.

We now write the expression for Δ^* as a function of Θ_1^* and Θ_2^* . Letting $M_{X_i} \succ 0$ denote the unique square root [11] of Σ_{X_i} , we can define $\tilde{Y}_i = M_{X_i} Y_i$ and take $\tilde{\Theta}_i^* = (\text{Cov}[\tilde{Y}_i])^{-1}$. Now, notice that with these definitions, we have

$$\Delta^* = M_{X_2} (\tilde{\Theta}_2^*)^{\frac{1}{2}} M_{X_2} - M_{X_1} (\tilde{\Theta}_1^*)^{\frac{1}{2}} M_{X_1}.$$

Consider the following “high-dimensional” estimator from [1]:

$$\hat{\Delta}_B \in \text{argmin}_{\Delta \in \mathbb{R}^{p \times p}} L(\Delta) + \lambda_n \|\Delta\|_{1, \text{off}}, \quad (1)$$

where $\lambda_n \geq 0$, and we define the loss function $L(\Delta)$ as follows:

$$L(\Delta) = \frac{1}{4} \left(\langle \hat{\Psi}_1 \Delta, \Delta \hat{\Psi}_2 \rangle + \langle \hat{\Psi}_2 \Delta, \Delta \hat{\Psi}_1 \rangle \right) - \langle \Delta, \hat{\Psi}_1 - \hat{\Psi}_2 \rangle, \quad (2)$$

where $\hat{\Psi}_i = M_{X_i}^{-1} \tilde{S}_i^{\frac{1}{2}} M_{X_i}^{-1}$ is an estimate of $\tilde{\Psi}_i = M_{X_i}^{-1} (\tilde{\Theta}_i^*)^{-\frac{1}{2}} M_{X_i}^{-1}$, S is the sample covariance matrix of \tilde{Y}_i . The term $\|\Delta\|_{1, \text{off}}$ represents the ℓ_1 -norm applied to the off-diagonal elements of Δ . This estimator is an ℓ_1 -regularized variant of the D-trace loss [8]. We also provide guarantees when injection vectors X_1 and X_2 follow other distributions in the paper, including those with polynomial tails.

3 Tail condition

We utilize the concept of tail condition from [2] to describe the distribution. This concept plays an important role in the central lemma of this paper.

Definition 1. Based on Ravikumar (Tail condition, [2]), the random vector Y satisfies the tail condition $T(f, v_*)$ if there exists a constant $v_* > 0$ and a function $f : \mathbb{N} \times (0, \infty) \rightarrow (0, \infty)$ such that for any $k, l \in [p]$ and $\delta \in (0, 1/v_*)$:

$$\mathbb{P} \left[|(\tilde{S}_i)_{kl} - (\tilde{\Theta}_i^{*-1})_{kl}| \geq \delta \right] \leq \frac{1}{f(n, \delta)} \quad (3)$$

$f(n, \delta)$ is monotonically increasing with respect to n or δ when the other variable is fixed. Two examples of tail functions f satisfy this monotone property are an exponential-type function, meaning that $f(n, \delta) = \exp(cn\delta^a)$, if $c, a > 0$, and a polynomial-type tail function meaning that $f(n, \delta) = cn^m \delta^{2m}$, for some positive integer m and scalar $c > 0$. The following inverse functions are required to show sample complexity,

$$n_f(\delta, r) := \max\{n : f(n, \delta) \leq p^n\} \quad \text{and} \quad \delta_f(n, r) := \max\{\delta : f(n, \delta) \leq p^n\}.$$

Since function $f(n, \delta)$ has the monotonicity property, the above functions are well defined and we know that if $n > n_f(\delta, p^\eta)$, this implies that $\delta \geq \delta_f(n, p^\eta)$.

3.1 Sub-Gaussian and Polynomial tail

Similar to the [8]. We study the case of sub-Gaussian and polynomial tail. We define the following

Definition 2 (Sub-Gaussian random variable). A mean-zero random vector $Z \in \mathbb{R}^p$ with covariance matrix Σ is called sub-Gaussian if there exists a constant $\sigma \in (0, \infty)$ such that

$$\mathbb{E} \left[\exp \left(t Z_i (\Sigma_{ii})^{-1/2} \right) \right] \leq \exp \left(\frac{\sigma^2 t^2}{2} \right),$$

for all $t \in \mathbb{R}$ and $i = 1, \dots, p$, where Σ_{ii} is the (i, i) element of Σ .

Based on the [2], if \tilde{Y}_i is *sub-Gaussian* with parameter σ . We have $v_* = \left\{ \max_i (\tilde{\Theta}^*)_{ii}^{-1} \cdot 8 (1 + 4\sigma^2) \right\}^{-1}$, and

$$f(n, \delta) = \frac{1}{4} \exp(-c_* n \delta^2), \quad \text{with } c_* = [128(1 + 4\delta^2)^2 \max_i (\tilde{\Theta}^*)_{ii}^{-1}]^{-1} \quad (4)$$

and the inverse functions take the form

$$\delta_f(p^\eta, n) = \sqrt{\frac{\log(4/p^\eta)}{c_* n}}, \quad \text{and} \quad n_f(p^\eta, \delta) = \frac{\log(4/p^\eta)}{c_* \delta^2}. \quad (5)$$

Definition 3 (Polynomial tail). A random vector $Z \in \mathbb{R}^p$ is said to have a polynomial tail if there exists a positive integer m and scalar $K_m \in \mathbb{R}$ such that

$$\mathbb{E} \left[\exp \left(t Z_i (\Sigma_{ii})^{-1/2} \right)^{4m} \right] \leq K_m,$$

for all $t \in \mathbb{R}$ and $i = 1, \dots, p$.

If \tilde{Y}_i is *polynomial tail* with parameter K_{1m} and K_{2m} respectively,

$$f(n, \delta) = c_k n^m \delta^{2m} \quad \text{where} \quad c_* = \frac{1}{(2m^2 + 12m^2 (\max_i (\tilde{\Theta}^*)_{ii}^{-1}))^2 m (K_m + 1)}, \quad (6)$$

and the inverse tail functions take the form,

$$\delta_f(n, p^\eta) = \left(\frac{p^\eta}{c_*} \right)^{\frac{1}{2m}} \frac{1}{\sqrt{n}}, \quad \text{and} \quad n_f(\delta, p^\eta) = \left(\frac{p^\eta}{c_*} \right)^{\frac{1}{m}} \frac{1}{\delta^2} \quad (7)$$

4 Statement of Main result

Our first result provides a theoretical analysis of the performance of estimator (1) when Y_1 and Y_2 follow a Sub-Gaussian distribution. In our setup, we assume that \tilde{Y}_i follow a Gaussian distribution. However, we work with sub-Gaussian distributions, which are a generalization of Gaussian distributions and include many common practical distributions. Additionally, we also extend this analysis to cases where Y_1 and Y_2 are non-Gaussian. Our results indicate that estimator (1) will reliably capture the sparsity structure of Δ^* and is close to the Δ^* with high probability as sample size n grows at a rate proportional to $p d^2 \log p$. Since our approach an ℓ_1 regularized variant of the D-trace loss function, the main result might appear similar to the [8]. However, In section 5.2.1, we discuss a novel challenge, which we refer to as the *Square Root Perturbation Bounds*. This challenge leads us to theorems that are not encompassed by previous work and opens a valuable avenue for future work.

We assume the true network difference Δ^* is sparse, that is, let $S = \{(i, j) : \Delta_{i,j}^* \neq 0\}$ be the support of Δ^* and $s = |S|$, $s < p$, d is the maximum number of non-zero entries across all rows in Δ^* , and $\max\{\|\tilde{\Psi}_1\|_\infty, \|\tilde{\Psi}_2\|_\infty\} \leq M$. We also define $\|A\|_1 = \|\text{vec}(A)\|_1$, $\|A\|_\infty = \max_{i,j} |A_{ij}|$ to denote the element-wise norm and in addition $\|A\|_{1,\infty} \triangleq \max_{i=1,\dots,p} \sum_{j=1}^p |A_{ij}|$, and $\kappa_\Gamma = \|\Gamma_{S,S}^*\|_{1,\infty}^{-1}$. Denote $\hat{\Gamma} = \frac{\tilde{\Psi}_1 \otimes \tilde{\Psi}_2 + \tilde{\Psi}_2 \otimes \tilde{\Psi}_1}{2}$ and $\Gamma^* = \frac{\tilde{\Psi}_1 \otimes \tilde{\Psi}_2 + \tilde{\Psi}_2 \otimes \tilde{\Psi}_1}{2}$. This is also the Hessian matrix for Δ of the D-trace loss function (2). We can consider that $\hat{\Gamma}$ could be used to describe the relationships between two sets of variables in this case could be for understanding the overall interaction between the two sets. For two subsets $T_1, T_2 \subseteq \{1, \dots, p\} \times \{1, \dots, p\}$, the submatrix of X , denoted by $X_{T_1 T_2}$, consists of rows and columns indexed by T_1 and T_2 , respectively. We begin with the required assumption.

Assumption 1. We assume the following irrepresentability condition

$$\max_{e \in S^c} \|\Gamma_{e,S}^* (\Gamma_{S,S}^*)^{-1}\|_1 \leq 1 - \alpha. \quad (8)$$

Where there are some $\alpha \in (0, 1]$

The Hessian $\Gamma_{(j,k),(l,m)}^*$ also shows the covariance of the random variable linked to each edge of the graph. This assumption is very similar to the one in [2], it imposes control on the influences that non-edge terms (indexed by S^c), can have on the edge-based terms (indexed by S).

The result of the converge rate is stated in terms of the tail function f , and its inverse n_f and δ_f . and The choices of λ is specified in terms of a user-defined parameter $\eta > 2$. larger choices of η yield a faster rate of convergence but lead to more stringent requirements on sample size.

Theorem 1. Let \tilde{Y}_1 and \tilde{Y}_2 be the node potential vector. Suppose that $\tilde{Y}_1/\sqrt{\tilde{\Theta}_{ii}^{*-1}}$ and $\tilde{Y}_2/\sqrt{\tilde{\Theta}_{ii}^{*-1}}$ are sub-Gaussian with parameter σ_1 and σ_2 , respectively. Under the irrepresentability condition (1) for some $\eta > 2$ and with a sample size for both \tilde{Y}_1 and \tilde{Y}_2 that is lower bounded as $n \geq p\tilde{C}_0(\eta \log(p) + \log(4))$, Then, with probability larger than $1 - 1/p^{\eta-2}$, for some $\eta > 2$:

- (a) $\hat{\Delta}$ recovers the sparsity structure of Δ^* ; that is, $\hat{\Delta}_{S^c} = 0$.
- (b) $\hat{\Delta}$ satisfies the element-wise ℓ_∞ bound $\|\hat{\Delta} - \Delta^*\|_\infty \leq \tilde{C}_1 \sqrt{p} \left[\frac{\eta \log(p) + \log(4)}{n} \right]^{\frac{1}{2}}$.

Where \tilde{C}_0 and \tilde{C}_1 are constant depending on κ_Γ, M, α , which we assume they remain constant as a function of n, p , and d . Specifically, for constant \tilde{C}_0 , can be simplified into $\mathcal{O}(d^2)$ (see Appendix A.2 for their definitions and detailed proof). Thus, we can have element-wise ℓ_∞ bound $\|\hat{\Delta} - \Delta^*\|_\infty \in \mathcal{O}(\sqrt{\frac{p \log(p)}{n}})$ with sample size $n = \Omega(pd^2 \log(p))$ holds with high probability. For the other quantities that are involved in the theorem statement, κ_Γ and M measure the size of the Hessian (Γ^{*-1}). Finally, both \tilde{C}_0 and \tilde{C}_1 also depend on the irrepresentability 1, which growing as the parameter α approaches 0.

Beyond the sub-Gaussian distribution, We also provide guarantees for other injection distributions with polynomial tails, making our approach applicable to a wider range of practical problems.

Corollary 1. Under the same condition and notation in Theorem 1 with probability greater than $1 - \frac{2}{p^{\eta-2}}$, When κ_Γ, M, α remain constant and the bound can be summarized as sample size $n = \Omega(pd^2 \log(p))$ can guarantee have the following rate in Frobenius and spectral norm for Exponential-type tails,

$$\|\hat{\Delta} - \Delta^*\|_F = \mathcal{O} \left(\sqrt{s+p} \sqrt{p} \left[\frac{\eta \log(p) + \log(4)}{n} \right]^{\frac{1}{2}} \right), \|\hat{\Delta} - \Delta^*\|_{op} = \mathcal{O} \left(\min\{\sqrt{s+p}, d\} \sqrt{p} \left[\frac{\eta \log(p) + \log(4)}{n} \right]^{\frac{1}{2}} \right).$$

Proof. The Frobenius and operator norm calculations follow directly from standard matrix norm inequalities applied to the element-wise ℓ_∞ bound in part (b) of Theorem 1. Details proof are provided in Appendix A.2.3. \square

Theorem 2. Under the same assumption of Theorem 1. Suppose that $\tilde{Y}_i/\sqrt{\tilde{\Theta}_{ii}^{*-1}}$ has bounded moment as in Definition 3 and with a sample size that is lower bounded as $n \geq p\tilde{C}_{P_0}^2(p^{\eta/m})$, Then, with probability larger than $1 - 2/p^{\eta-2}$, for some $\eta > 2$:

- (a) $\hat{\Delta}$ recovers the sparsity structure of Δ^* ; that is, $\hat{\Delta}_{S^c} = 0$.
- (b) $\hat{\Delta}$ satisfies the element-wise ℓ_∞ bound $\|\hat{\Delta} - \Delta^*\|_\infty \leq \tilde{C}_{P_1} \sqrt{p} \left[\frac{p^{\eta/m}}{n} \right]^{\frac{1}{2}}$.

Similar to Theorem 1, \tilde{C}_{P_0} and \tilde{C}_{P_1} are constant depending on κ_Γ, M, α , which we assume they remain constant as a function of n, p , and d . We can have element-wise ℓ_∞ bound $\|\hat{\Delta} - \Delta^*\|_\infty \in \mathcal{O}(\sqrt{p} \sqrt{\frac{p^{\eta/m}}{n}})$ with sample size $n = \Omega(pd^2 p^{\eta/m})$ holds with high probability.

Corollary 2. Under the assumption in the Theorem 2, we have the following rate in Frobenius and spectral norm for Polynomial-type tails

$$\|\hat{\Delta} - \Delta^*\|_F = \mathcal{O} \left(\sqrt{s+p} \sqrt{p} \left[\frac{p^{\eta/m}}{n} \right]^{\frac{1}{2}} \right), \|\hat{\Delta} - \Delta^*\|_{op} = \mathcal{O} \left(\min\{\sqrt{s+p}, d\} \sqrt{p} \left[\frac{p^{\eta/m}}{n} \right]^{\frac{1}{2}} \right).$$

Proof. Similar to the previous proof, detailed proof are provided in Appendix A.2.3. \square

5 Proofs Outline of Main Result

Our proof builds on the *primal-dual witness* framework established in [2]. The method involves constructing a *primal-dual witness* pair $(\tilde{\Delta}, \tilde{Z})$ that satisfies the optimality conditions of our problem (1). If the construction succeeds, then $\tilde{\Delta} = \hat{\Delta}$. Thus, the main direction of our proof is to demonstrate that this construction succeeds with high probability.

While developing our proof, we encountered an interesting challenge: the *square root perturbation bound* problem. We address this issue to derive statistical guarantees for our convex estimator in (1). First, we construct the *primal-dual witness method* and then provide a sequence of lemmas establishing the necessary conditions for the method to hold. Finally, we show that all conditions are satisfied under the assumptions specified in Theorems 1 and 2.

5.1 Primal-Dual witness method

We construct a *Primal-dual witness* pair $(\tilde{\Delta}, \tilde{Z})$ as following. The $\tilde{\Delta}$ is the solution to the restrictive problem:

$$\tilde{\Delta} = \arg \min_{\Delta \in \mathbb{R}^{p \times p}, \Delta_{S^c} = 0} L(\Delta) + \lambda_n \|\Delta\|_{1, \text{off}} \quad (9)$$

We note that the sub-differential of $\|\cdot\|_{1, \text{off}}$ with respect of Δ contains set of matrices $Z \in \mathbb{R}^{p \times p}$ such that

$$Z_{ij} = \begin{cases} 0, & \text{if } i = j \\ \text{sign}(\Delta_{ij}), & \text{if } i \neq j \text{ and } \Delta_{ij} \neq 0 \\ \in [-1, +1], & \text{if } i \neq j \text{ and } \Delta_{ij} = 0 \end{cases} \quad (10)$$

The $\tilde{\Delta}$ in the sub-differential of $\|\Delta\|_{1, \text{off}}$ is chosen so it satisfies the optimality condition of (9). This can be done by setting \tilde{Z}_{S^c} as

$$\tilde{Z}_{S^c} = -\frac{1}{\lambda_n} \left\{ \frac{1}{2} (\hat{\Psi}_1 \tilde{\Delta} \hat{\Psi}_2 + \hat{\Psi}_2 \tilde{\Delta} \hat{\Psi}_1) - \hat{\Psi}_1 + \hat{\Psi}_2 \right\}_{S^c}$$

Finally, we need to establish the *strict dual feasibility*

$$|\tilde{Z}_{ij}| < 1, \text{ For all } (i, j)$$

5.2 Supporting Results and Lemmas

The proof of theorem 1 and 2 requires a sequence of lemmas. We further define the following notations.

$$\epsilon = \|\widehat{\Psi}_1 - \widetilde{\Psi}_1\|_\infty \|\widehat{\Psi}_2 - \widetilde{\Psi}_2\|_\infty + \|\widetilde{\Psi}_1\|_\infty \|\widehat{\Psi}_2 - \widetilde{\Psi}_2\|_\infty + \|\widetilde{\Psi}_2\|_\infty \|\widehat{\Psi}_1 - \widetilde{\Psi}_1\|_\infty,$$

$$\tilde{\epsilon} = \|\widehat{\Psi}_1 - \widehat{\Psi}_2 - \widetilde{\Psi}_1 + \widetilde{\Psi}_2\|_\infty, \Delta_\Gamma = \hat{\Gamma} - \Gamma^*.$$

Let $R(\Delta_\Gamma)$ denote the difference of gradient $\nabla g(\hat{\Gamma}_{S,S})$ from its first-order Taylor expansion around $\Gamma_{S,S}^*$, we obtain the remainder takes the form

$$R(\Delta_\Gamma) = \hat{\Gamma}_{S,S}^{-1} - \Gamma_{S,S}^{*-1} + \Gamma_{S,S}^{*-1}(\Delta_\Gamma)_{S,S}\Gamma_{S,S}^{*-1}.$$

In this section, we first provide conditions for the *strict dual feasibility condition* to hold. Then, we control the remainder term $R(\Delta_\Gamma)$, providing element-wise error bounds on $\hat{\Delta}$ and Δ^* in terms of ϵ . Finally, we show that with an appropriate choice of λ_n and under the sample size bounded as stated in Theorem 1 and 2, all conditions for the *strict dual feasibility condition* are satisfied, and the proof of the final result can be done by applying the *Square Root Perturbation Bounds*.

Lemma 1 (Conditions for strict dual feasibility and error bound). Let the regularization parameter $\lambda_n > 0$, and assume that Assumption 1 holds. If the following conditions are satisfied:

(i) $\hat{\Delta}_{S^c} = 0$, if

$$\max_{e \in S^c} \|\hat{\Gamma}_{e,S}(\hat{\Gamma}_{S,S})^{-1}\|_1 \leq 1 - \alpha/2, \quad \|\hat{\Gamma}_{e,S}(\hat{\Gamma}_{S,S})^{-1} - \Gamma_{e,S}^*(\Gamma_{S,S}^*)^{-1}\|_1 \leq \frac{\alpha\lambda_n}{8M}, \quad (11)$$

$$\tilde{\epsilon} \leq \frac{\alpha\lambda_n}{2(4-\alpha)}; \quad (12)$$

(ii) $\hat{\Delta}_{S^c} = 0$, if

$$\epsilon < \frac{1}{6s\kappa_\Gamma}, \quad (13)$$

$$3s\epsilon(\kappa_\Gamma + 2sM^2\kappa_\Gamma^2) \leq 0.5\alpha \min(1, 0.25\lambda_n M^{-1}), \quad (14)$$

$$\tilde{\epsilon} \leq \frac{\alpha\lambda_n}{2(4-\alpha)}; \quad (15)$$

(iii) Under the conditions in (ii), we also have

$$\|\hat{\Delta} - \Delta^*\|_\infty < (\tilde{\epsilon} + \lambda_n)\kappa_\Gamma + 3(\tilde{\epsilon} + 2M + \lambda_n)s\epsilon\kappa_\Gamma^2. \quad (16)$$

Proof. Since the proofs are very similar to the [8], we only provide a high-level picture of our proofs. It is divided into three parts corresponding to (i), (ii), and (iii). Part (i) establishes the condition for the *primal-dual witness* to hold. Part (ii) builds the connection between (i) and (iii), while part (iii) provides the error bound necessary for our central lemma, which will be discussed later.

For part (i), we establish that the *Primal-Dual Witness* holds under the conditions stated in Lemma 1. Specifically, we follow the proof of Lemma A1 in the Supplementary Material of [8] to verify that the inequality below implies the two inequalities in (11):

$$\max_{e \in S^c} \left\| \hat{\Gamma}_{e,S} \left(\hat{\Gamma}_{S,S} \right)^{-1} - \Gamma_{e,S}^* \left(\Gamma_{S,S}^* \right)^{-1} \right\|_1 \leq 0.5\alpha \min(1, 0.25\lambda_n M^{-1}). \quad (17)$$

The second inequality in (11) follows directly from (17). To prove the first inequality, we combine the fact that $\alpha = 1 - \max_{e \in S^c} \|\Gamma_{e,S}^*(\Gamma_{S,S}^*)^{-1}\|_1$ and apply the triangle inequality.

For part (ii), we can see that the right-hand side of (17) is equivalent to the right-hand side of (14). Therefore, it suffices to show that the left-hand side of (17) is smaller than the left-hand side of (14). This follows the same reasoning as in the proof of Lemma A1 in [8], with adjustments to match our notation. Specifically, Σ_X^* and Σ_Y^* in [8] are replaced with $\tilde{\Psi}_1$ and $\tilde{\Psi}_2$, respectively, while $\hat{\Sigma}_X$ and $\hat{\Sigma}_Y$ are replaced with $\hat{\Psi}_1$ and $\hat{\Psi}_2$. Apart from this notational change, the argument remains consistent with the original proof. We will later verify all conditions in part (ii) with a sample size lower-bounded as specified in Theorems 1 and 2 within the proof of the central Lemma.

For part (iii), using the inequalities from (iii) and Lemma 2, which is stated right after, we obtain the inequality (16). See the proofs of Lemmas A1 and A2 in [8] for further details. \square

Lemma 2. (control of remainder) Combine condition 13 from Lemma 1 and we get $\|\Gamma_{S,S}^{*-1}\|_{1,\infty} \|(\Delta_\Gamma)_{S,S}\|_{1,\infty} < \frac{1}{3}$. Then,

$$\|R(\Delta_\Gamma)\|_\infty \leq 6d\epsilon^2\kappa_\Gamma^3, \|R(\Delta_\Gamma)\|_{1,\infty} \leq 6d^2\epsilon^2\kappa_\Gamma^3 \quad (18)$$

Since $R(\Delta_\Gamma) = \hat{\Gamma}_{S,S}^{-1} - \Gamma_{S,S}^{*-1} + \Gamma_{S,S}^{*-1}(\Delta_\Gamma)_{S,S}\Gamma_{S,S}^{*-1}$. We have

$$\|\hat{\Gamma}_{S,S}^{-1} - \Gamma_{S,S}^{*-1}\|_\infty \leq 6d\epsilon^2\kappa_\Gamma^3 + 2\epsilon\kappa_\Gamma^2 \quad (19)$$

$$\|\hat{\Gamma}_{S,S}^{-1} - \Gamma_{S,S}^{*-1}\|_{1,\infty} \leq 6d^2\epsilon^2\kappa_\Gamma^3 + 2d\epsilon\kappa_\Gamma^2 \quad (20)$$

Proof. The proof of this follows the same approach as Lemmas A2 in the Supplementary Material of [8]. \square

5.2.1 Square Root Perturbation Bounds

The estimator (1) use $\hat{\Psi}_i$ as proxy for the true $\tilde{\Psi}_i$. The first step is to obtain bounds on the differences $\hat{\Psi}_i - \tilde{\Psi}_i$, which can be written as $M_{X_i}^{-1} \left(\tilde{S}_i^{\frac{1}{2}} - (\tilde{\Theta}_i^*)^{-\frac{1}{2}} \right) M_{X_i}^{-1}$. To bound the differences $\tilde{S}_i^{\frac{1}{2}} - (\tilde{\Theta}_i^*)^{-\frac{1}{2}}$, we need to identify alternative expressions that bound the behavior of the square root function.

Lemma 3. (Generalized Power-Stormer Inequalities [12]) Let A and B be positive operators and let $n \geq 1$. If f is an operator monotone function. Then,

$$\|A^{\frac{1}{n}} - B^{\frac{1}{n}}\|_{op} \leq \|A - B\|_{op}^{\frac{1}{n}}$$

From Lemma 3 we can obtain the following chain of inequality,

$$\|\sqrt{S_i} - \sqrt{\Theta_i^{*-1}}\|_\infty \leq \|\sqrt{S_i} - \sqrt{\Theta_i^{*-1}}\|_{op} \leq \sqrt{\|S_i - \Theta_i^{*-1}\|_{op}} \leq \sqrt{p} \|S_i - \Theta_i^{*-1}\|_\infty$$

Instead of direct calculation on the $\tilde{S}_i^{\frac{1}{2}} - (\tilde{\Theta}_i^*)^{-\frac{1}{2}}$, now we can use $\sqrt{p} \|\tilde{S}_i - \tilde{\Theta}_i^{*-1}\|_\infty$ to have bounds on the differences $\tilde{S}_i - (\tilde{\Theta}_i^*)^{-1}$. The final result of the Theorem 1 and 2 is based on the the control of noise $\hat{\Psi}_i - \tilde{\Psi}_i$. We have inequality:

$$\|\hat{\Psi}_i - \tilde{\Psi}_i\|_\infty = \|M_{X_i}^{-1}\|_\infty \|(\tilde{S}_i)^{\frac{1}{2}} - (\tilde{\Theta}_i^*)^{-\frac{1}{2}}\|_\infty \|M_{X_i}^{-1}\|_\infty \leq \|M_{X_i}^{-1}\|_\infty \sqrt{p} \|\tilde{S}_i - (\tilde{\Theta}_i^*)^{-1}\|_\infty \|M_{X_i}^{-1}\|_\infty \quad (21)$$

Lemma 4. (Control of noise term) Let $\tilde{\delta}_{f_i} = \|M_{X_i}^{-1}\|_\infty \sqrt{p} \delta_{f_i}(n, p^n) \|M_{X_i}^{-1}\|_\infty$. For some $\eta > 2$, We have

$$\mathbb{P} \left(\|\hat{\Psi}_i - \tilde{\Psi}_i\|_\infty \leq \tilde{\delta}_{f_i}(n, p^n) \right) \geq 1 - \frac{1}{p^{\eta-2}},$$

Proof. For any $0 < \delta < 1/v_*$ and $r \geq 1$, if $n > n_f(\delta, r)$, we have $f(n, \delta) > r$ and thus $\delta_f(n, r) < \delta$, since $f(n, \delta)$ is monotonically increasing in δ . Thus $\mathbb{P}\{|\tilde{S}_i - (\tilde{\Theta}_i^*)^{-1}| \geq \delta_f(n, r)\} \leq 1/f(n, \delta_f(n, r)) = r^{-1}$, applying union bound across all entries, we have $\mathbb{P}\{\|\tilde{S}_i - (\tilde{\Theta}_i^*)^{-1}\|_\infty < \delta_f(n, r)\} > 1 - p^2 r^{-1}$. Finally, apply the inequalities (21), and set $r = p^\tau$. We obtain

$$\mathbb{P}\left(\|M_{X_i}^{-1}\|_\infty \sqrt{p} \|\tilde{S}_i - (\tilde{\Theta}_i^*)^{-1}\|_\infty \|M_{X_i}^{-1}\|_\infty \leq \|M_{X_i}^{-1}\|_\infty \sqrt{p} \delta_f(n, p^\tau) \|M_{X_i}^{-1}\|_\infty\right) \geq 1 - \frac{1}{p^{\tau-2}}. \quad (22)$$

□

We now need to offer guarantees for support recovery and bounds for the infinity norm of $\hat{\Delta}$ for distribution that comply with the tail condition $T(f, v_*)$ as outlined in the Definition 1.

Lemma 5. (Central Lemma) let $\hat{\Delta}$ be the unique solution of the problem 1 with

$$\lambda_n = \max\left\{\frac{2(4-\alpha)(\tilde{\delta}_{f_1} + \tilde{\delta}_{f_2})}{\alpha}, \frac{24dM(\kappa_\Gamma + dM^2\kappa_\Gamma^2)(\tilde{\delta}_{f_1}\tilde{\delta}_{f_2} + M\tilde{\delta}_{f_2} + M\tilde{\delta}_{f_1})}{\alpha}\right\}.$$

For a distribution satisfying the assumption 1 and the tail condition $T(f, v_*)$ in 1. Then if the sample size is lower bounded as

$$n > n_f\left(\min\left\{-M + \sqrt{M^2 + (6d\kappa_\Gamma)^{-1}}, -M + \sqrt{M^2 + \frac{\alpha}{24d(\kappa_\Gamma + dM^2\kappa_\Gamma^2)}}, \frac{\alpha M}{4-\alpha}\right\}, p^\tau\right)$$

then with probability greater than $1 - \frac{1}{p^{\tau-2}}$, the $\hat{\Delta}$ recovers the sparsity structure of Δ^* , and satisfies the ℓ_∞ bound

$$\|\hat{\Delta} - \Delta^*\|_\infty \leq (\tilde{\delta}_{f_1} + \tilde{\delta}_{f_2} + \lambda_n)\kappa_\Gamma + 3d\kappa_\Gamma^2(\tilde{\delta}_{f_1} + \tilde{\delta}_{f_2} + \lambda_n + 2M)(\tilde{\delta}_{f_1}\tilde{\delta}_{f_2} + M\tilde{\delta}_{f_2} + M\tilde{\delta}_{f_1}) \quad (23)$$

Proof Sketch. We show that the Primal-Dual witness construction succeeds (see proof of Lemma 1 and 2) with the probability and information stated in this Lemma, This is equivalent to demonstrating that the inequalities in Lemma 1 holds with the required probability. We have show that $\mathbb{P}\left(\|\hat{\Psi}_i - \tilde{\Psi}_i\|_\infty \leq \tilde{\delta}_{f_i}(n, p^\tau)\right) \geq 1 - \frac{1}{p^{\tau-2}}$, in Lemma 4. Given that event $\|\hat{\Psi}_i - \tilde{\Psi}_i\|_\infty \leq \tilde{\delta}_{f_i}(n, p^\tau)$ holds, we then demonstrate that the inequalities in 1 are satisfied. We provide full proof in Appendix A.1.

The result in Theorem 1 and 2 follow by combining those sequence of lemmas. Substituting inverse functions of *Sub-Gaussian* and *Polynomial tail* in 1 to 23, we obtain δ_{f_1} and δ_{f_2} . Finally, the main result is proved by applying some algebraic manipulations to (23).

6 Numerical Simulations

In this section, we provided multiple simulations to show the performance of our estimator on synthetic and benchmark networks. It should be noted that for the sub-Gaussian random variable, while the sample complexity scales like $pd^2 \log p$, one might hope it would scale like $d^2 \log p$, since in this way, the sample size required can be substantially smaller than the graph size, since in practice the maximum node degrees, d normally behave $d = o(p)$ or stay as a constant. This scaling shows the estimator can success in the "large p small n " setting. Thus, to further explode our estimator efficiency under this setting, we plot the learning accuracy and error norm of the estimator as the scaled sample size $n/(d^2 \log(p))$ instead of what the theoretical result in Theorem 1 and 2, which suggest $pd^2 \log p$.

6.1 Experiment set up

Our experiment mainly focuses on recovering the correct sparsity structure of Δ^* and norm consistency. we use the F1-score and the Frobenius norm of the error $\|\hat{\Delta} - \Delta^*\|_F$ for all experiments. We also set the $\lambda_n \propto \sqrt{\log(p)/n}$.

6.2 Synthetic networks

In this section, we conduct simulations to evaluate the performance of the proposed estimator on four different kinds of synthetic random networks. All synthetic networks have the same size of $p = 30$. In figure 1 we show the estimate accuracy and error norm for different choices of Δ^* whose underlying graphs are Erdős-Rényi, Small-World (Watts-Strogatz model), and Scale-Free (Barabási-Albert model), and synthetic grid graph with corresponding maximum degrees $d = \{5, 6, 16, 7\}$ respectively.

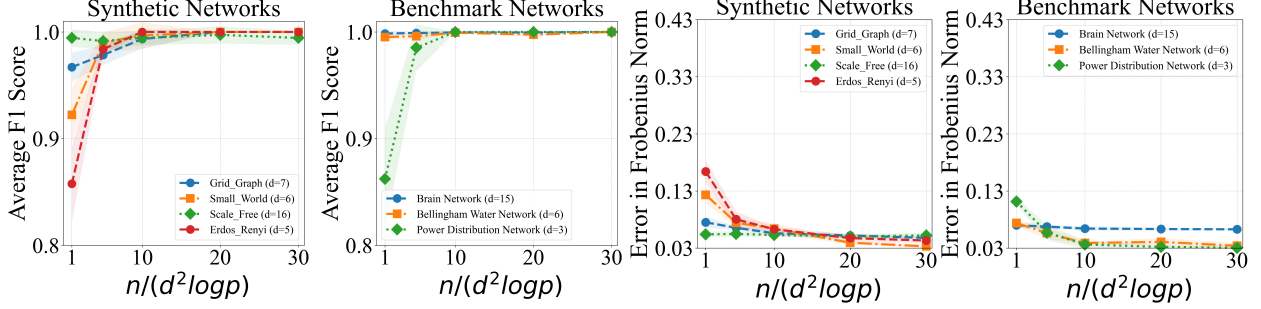


Figure 1: Estimation Accuracy.

6.3 Benchmark networks

1. **Power distribution network:** We analyze the IEEE 33-bus power distribution network. The raw data file are accessible¹. This network comprises 33 buses and 32 branches (edges), with a maximum degree of $d = 3$. The adjacency matrix A contains both positive and negative eigenvalues.
2. **Water distribution network:** The ground truth adjacency matrix, with 121 nodes and 162 edges and maximum degree of $d = 6$, is generated by loading the raw data described in [13] into the WNTR simulator². The raw data file are accessible³.
3. **Brain network:** The benchmark connectivity (adjacency) matrix used in this study is publicly available⁴, with a comprehensive explanation of its construction provided in [14]. The ground truth adjacency matrix, denoted A , is a 90×90 matrix (representing 90 nodes), where each row and column corresponds to a distinct region of interest (ROI) in the brain.

7 Discussion and Future Work

Our simulation in supports recovery for high-dimensional data, demonstrating results that imply a sample complexity scaling as $\mathcal{O}(d^2 \log(p))$. This scaling is sublinear in the dimension p , Which means that our method works well even when $n < p$. However, our theoretical analysis to date has only managed to establish a sample complexity $\mathcal{O}(pd^2 \log(p))$. Closing this gap between theory and simulation is a primary objective for our future research. The main problem with having a less strong bound comes from the challenge of looking for concentration inequality for the square root of the matrix.

¹<https://www.mathworks.com/matlabcentral/fileexchange/73127-ieee-33-bus-system>

²<https://github.com/USEPA/WNTR>

³<https://www.uky.edu/WDST/index.html>

⁴<https://osf.io/yw5vf/>

References

- [1] Anirudh Rayas, Rajasekhar Anguluri, Jiajun Cheng, and Gautam Dasarathy. Differential analysis for networks obeying conservation laws. In *ICASSP 2023-2023 IEEE International Conference on Acoustics, Speech and Signal Processing (ICASSP)*, pages 1–5. IEEE, 2023.
- [2] Pradeep Ravikumar, Martin J Wainwright, Garvesh Raskutti, and Bin Yu. High-dimensional covariance estimation by minimizing ℓ_1 -penalized log-determinant divergence. *Electronic Journal of Statistics*, 22: 935–980, 2011.
- [3] Anirudh Rayas, Rajasekhar Anguluri, and Gautam Dasarathy. Learning the structure of large networked systems obeying conservation laws. In *Advances in Neural Information Processing Systems*, volume 35, pages 14637–14650. Curran Associates, Inc., 2022.
- [4] Rajasekhar Anguluri, Gautam Dasarathy, Oliver Kosut, and Lalitha Sankar. Grid topology identification with hidden nodes via structured norm minimization. *IEEE Control Systems Letters*, 6:1244–1249, 2021.
- [5] Deepjyoti Deka, Saurav Talukdar, Michael Chertkov, and Murti V Salapaka. Graphical models in meshed distribution grids: Topology estimation, change detection & limitations. *IEEE Transactions on Smart Grid*, 11(5):4299–4310, 2020.
- [6] Ali Shojaie. Differential network analysis: A statistical perspective. *Wiley Interdisciplinary Reviews: Computational Statistics*, 13(2), 2021.
- [7] Sen Na, Mladen Kolar, and Oluwasanmi Koyejo. Estimating differential latent variable graphical models with applications to brain connectivity. *Biometrika*, 108(2):425–442, 2021.
- [8] Huili Yuan, Ruibin Xi, Chong Chen, and Minghua Deng. Differential network analysis via lasso penalized D-trace loss. *Biometrika*, 104(4):755–770, 2017.
- [9] Gautam Dasarathy, Parikshit Shah, and Richard G Baraniuk. Sketched covariance testing: A compression-statistics tradeoff. In *2017 51st Asilomar Conference on Signals, Systems, and Computers*, pages 676–680. IEEE, 2017.
- [10] Teng Zhang and Hui Zou. Sparse precision matrix estimation via lasso penalized D-trace loss. *Biometrika*, 101(1):103–120, 2014.
- [11] Rajendra Bhatia. Positive definite matrices. Princeton University Press, 2009.
- [12] John Phillips. On the uniform continuity of operator functions and generalized powers-stormer inequalities. 1987. URL <http://hdl.handle.net/1828/1506>. Available since 2009-08-14T17:19:22Z.
- [13] Erika Hernandez, Steven Hoagland, and Lindell Ormsbee. Water distribution database for research applications. In *World Environmental and Water Resources Congress*, pages 465–474, 2016.
- [14] Antonín Škoch, Barbora Reháková, Jan Mareš, Jaroslav Tintěra, Pavel Sanda, Lucia Jajcay, Jiří Horáček, Filip Španiel, and Jaroslav Hlinka. Human brain structural connectivity matrices—ready for modelling. *Scientific Data*, 9(1), 2022.

A Appendix

For clarity, we recall the following definitions.

$$\begin{aligned}\epsilon &= \|\widehat{\Psi}_1 - \widetilde{\Psi}_1\|_\infty \|\widehat{\Psi}_2 - \widetilde{\Psi}_2\|_\infty + \|\widetilde{\Psi}_1\|_\infty \|\widehat{\Psi}_2 - \widetilde{\Psi}_2\|_\infty + \|\widetilde{\Psi}_2\|_\infty \|\widehat{\Psi}_1 - \widetilde{\Psi}_1\|_\infty, \\ \tilde{\epsilon} &= \|\widehat{\Psi}_1 - \widehat{\Psi}_2 - \widetilde{\Psi}_1 + \widetilde{\Psi}_2\|_\infty.\end{aligned}$$

A.1 Proof of Lemma 5

Let

$$\begin{aligned}\bar{\delta} &= \min\{-M + \sqrt{M^2 + (6d\kappa_\Gamma)^{-1}}, -M + \sqrt{M^2 + \frac{\alpha}{24d(\kappa_\Gamma + dM^2\kappa_\Gamma^2)}}, \frac{\alpha M}{4 - \alpha}\}, \\ \lambda_n &= \max\left\{\frac{2(4 - \alpha)(\widetilde{\delta}_{f_1} + \widetilde{\delta}_{f_2})}{\alpha}, \frac{24dM(\kappa_\Gamma + dM^2\kappa_\Gamma^2)(\widetilde{\delta}_{f_1}\widetilde{\delta}_{f_2} + M\widetilde{\delta}_{f_2} + M\widetilde{\delta}_{f_1})}{\alpha}\right\}.\end{aligned}$$

For $n > n_f(\bar{\delta}, p^\eta)$, the following hold with probability at least $1 - 1/p^{\eta-2}$, we have

$$\begin{aligned}\|\widehat{\Psi}_1 - \widetilde{\Psi}_1\|_\infty &\leq \widetilde{\delta}_{f_1}(n_1, p^\eta) = \widetilde{\delta}_{f_1} < \bar{\delta}, \\ \|\widehat{\Psi}_2 - \widetilde{\Psi}_2\|_\infty &\leq \widetilde{\delta}_{f_2}(n_2, p^\eta) = \widetilde{\delta}_{f_2} < \bar{\delta}.\end{aligned}$$

we now prove our *Central Lemma* in the following steps. First we verify all conditions in part (ii) of Lemma 1. Since $\epsilon \leq \widetilde{\delta}_{f_1}\widetilde{\delta}_{f_2} + M\widetilde{\delta}_{f_2} + M\widetilde{\delta}_{f_1} < \bar{\delta}^2 + 2M\bar{\delta}$ and $\bar{\delta} = -M + \sqrt{M^2 + (6d\kappa_\Gamma)^{-1}}$, condition (13) can be easily verified. From $\delta_{f_1} < \bar{\delta} \leq -M + \sqrt{M^2 + \frac{\alpha}{24d(\kappa_\Gamma + dM^2\kappa_\Gamma^2)}}$, we get $\epsilon \leq \delta_{f_1}\delta_{f_2} + M\delta_{f_2} + M\delta_{f_1} \leq \frac{\alpha}{24d(\kappa_\Gamma + dM^2\kappa_\Gamma^2)}$, which implies that $3d\epsilon(\kappa_\Gamma + dM^2\kappa_\Gamma^2) \leq \alpha/8 < \alpha/2$. Since $\widetilde{\delta}_{f_1} = \widetilde{\delta}_{f_1}(n_1, p^\eta) < \bar{\delta} \leq \frac{\alpha M}{4 - \alpha}$, $\widetilde{\delta}_{f_2} = \widetilde{\delta}_{f_2}(n_2, p^\eta) < \bar{\delta} \leq \frac{\alpha M}{4 - \alpha}$, now we have $\frac{2(4 - \alpha)(\widetilde{\delta}_{f_1} + \widetilde{\delta}_{f_2})}{\alpha} \leq 4M$. Then, Recall the condition (14) we have definition of λ_n , $0.25M^{-1}\lambda_n \leq 1$. Now we have,

$$\begin{aligned}3d\epsilon(\kappa_\Gamma + dM^2\kappa_\Gamma^2) &\leq 3d(\kappa_\Gamma + dM^2\kappa_\Gamma^2)(\widetilde{\delta}_{f_1}\widetilde{\delta}_{f_2} + M\widetilde{\delta}_{f_2} + M\widetilde{\delta}_{f_1}) \\ &= 8^{-1}\alpha M^{-1} \frac{24dM(\kappa_\Gamma + dM^2\kappa_\Gamma^2)(\widetilde{\delta}_{f_1}\widetilde{\delta}_{f_2} + M\widetilde{\delta}_{f_2} + M\widetilde{\delta}_{f_1})}{\alpha} \\ &\leq 8^{-1}\alpha M^{-1}\lambda_n.\end{aligned}$$

Combining the above results, condition (14) is verified. The condition (15) can be verified as following,

$$\tilde{\epsilon} \leq \|\widehat{\Psi}_1 - \widetilde{\Psi}_1\|_\infty + \|\widehat{\Psi}_2 - \widetilde{\Psi}_2\|_\infty \leq (\widetilde{\delta}_{f_1} + \widetilde{\delta}_{f_2}) \leq \frac{\alpha\lambda_n}{2(4 - \alpha)}.$$

A.2 Proof of Theorem 1 and Theorem 2

Then, by part (iii) of the Lemma 1, We have

$$\begin{aligned}\|\widehat{\Delta} - \Delta^*\|_\infty &< (\hat{\epsilon} + \lambda_n)\kappa_\Gamma + 3(\hat{\epsilon} + 2M + \lambda_n)d\epsilon\kappa_\Gamma^2 \\ &\leq (\widetilde{\delta}_{f_1} + \widetilde{\delta}_{f_2} + \lambda_n)\kappa_\Gamma + 3d\kappa_\Gamma^2(\widetilde{\delta}_{f_1} + \widetilde{\delta}_{f_2} + \lambda_n + 2M)(\widetilde{\delta}_{f_1}\widetilde{\delta}_{f_2} + M\widetilde{\delta}_{f_2} + M\widetilde{\delta}_{f_1}).\end{aligned}\tag{24}$$

A.2.1 Theorem 1

Suppose that \tilde{Y}_1 and \tilde{Y}_2 are sub-Gaussian,

Part(a): From Lemma 5, we show that if $n > n_f(\delta, p^\eta)$, then $\hat{\Delta}$ recovers the sparsity structure of Δ^* . we use the tail condition for sub-gaussian distributions and inverse functions from 1 we have

$$\tilde{n}_f(\delta, p^\eta) = \min \left\{ -M + \sqrt{M^2 + (6d\kappa_\Gamma)^{-1}}, -M + \sqrt{M^2 + \frac{\alpha}{24d(\kappa_\Gamma + dM^2\kappa_\Gamma^2)}}, \frac{\alpha M}{16} \right\}^{-2} p\tilde{C}^2(\eta \log(p) + \log(4))$$

Where $\tilde{C} = 128[1 + 4\max(\sigma_1^2, \sigma_2^2)\max(\max_i((\Theta_1^{*-1})_{ii}), \max_i((\Theta_2^{*-1})_{ii}))^2]^{\frac{1}{4}} \max(\|M_{X_1}^{-1}\|_\infty^2, \|M_{X_2}^{-1}\|_\infty^2)$. We can conclude that if

$$n \geq \min \left\{ -M + \sqrt{M^2 + (6d\kappa_\Gamma)^{-1}}, -M + \sqrt{M^2 + \frac{\alpha}{24d(\kappa_\Gamma + dM^2\kappa_\Gamma^2)}}, \frac{\alpha M}{16} \right\}^{-2} p\tilde{C}^2(\eta \log(p) + \log(4)),$$

the estimator $\hat{\Delta}$ recovers the sparsity structure of Δ^* .

$$\tilde{C} = 128 \left(1 + 4\max(\sigma_1^2, \sigma_2^2)\max\{\max_i\{(\tilde{\Theta}_1^{*-1})_{ii}\}, \max_i\{(\tilde{\Theta}_2^{*-1})_{ii}\}\}^2 \right)^{\frac{1}{4}} \max\{\|M_{X_1}^{-1}\|_\infty^2, \|M_{X_2}^{-1}\|_\infty^2\}.$$

if we assume that M, κ_Γ , and α are constant as functions of n, p, d , the above expression can be simplified into $n = \Omega(d^2 p \log(p))$.

Part(b) : Compute $\tilde{\delta}_{f_i}$ based on the definition 1, we obtain

$$\tilde{\delta}_{f_1} \leq [128(1 + 4\sigma_1^2)\max_i((\tilde{\Theta}_1^{*-1})_{ii})^2]^{\frac{1}{4}} \|M_{X_1}^{-1}\|_\infty^2 p^{\frac{1}{2}} \left\{ \frac{\eta \log(p) + \log(4)}{n} \right\}^{\frac{1}{2}}$$

$$\tilde{\delta}_{f_2} \leq [128(1 + 4\sigma_2^2)\max_i((\tilde{\Theta}_2^{*-1})_{ii})^2]^{\frac{1}{4}} \|M_{X_2}^{-1}\|_\infty^2 p^{\frac{1}{2}} \left\{ \frac{\eta \log(p) + \log(4)}{n} \right\}^{\frac{1}{2}}$$

The main result in Theorem 1 can now be proved by substituting the above inequalities into the right-hand side of equation 24 with some algebra manipulation. Finally we obtain

$$\begin{aligned} \|\hat{\Delta} - \Delta^*\|_\infty &\leq \left[\kappa_\Gamma + 3d\kappa_\Gamma^2 M^2 \left(\frac{\alpha^2}{256} + \frac{\alpha}{8} \right) \right] \left[2\tilde{C} + \max \left\{ \frac{8\tilde{C}}{\alpha}, \left(\frac{6}{16} + \frac{32}{\alpha} \right) dM^2(\kappa_\Gamma + dM^2\kappa_\Gamma^2) \right\} \right] \\ &\quad + \left[\frac{6}{16} dM^2\kappa_\Gamma^2(\alpha + 32)\tilde{C} \right] \sqrt{p} \left[\frac{\eta \log(p) + \log(4)}{n} \right]^{\frac{1}{2}}. \end{aligned}$$

Let \tilde{C}_0 be defined as

$$\min \left\{ -M + \sqrt{M^2 + (6d\kappa_\Gamma)^{-1}}, -M + \sqrt{M^2 + \frac{\alpha}{24d(\kappa_\Gamma + dM^2\kappa_\Gamma^2)}}, \frac{\alpha M}{16} \right\}^{-2} p\tilde{C}^2,$$

and \tilde{C}_1 be defined as

$$\left[\kappa_\Gamma + 3d\kappa_\Gamma^2 M^2 \left(\frac{\alpha^2}{256} + \frac{\alpha}{8} \right) \right] \left[2\tilde{C} + \max \left\{ \frac{8\tilde{C}}{\alpha}, \left(\frac{6}{16} + \frac{32}{\alpha} \right) dM^2(\kappa_\Gamma + dM^2\kappa_\Gamma^2) \right\} \right] + \left[\frac{6}{16} dM^2\kappa_\Gamma^2(\alpha + 32)\tilde{C} \right].$$

This completes the proof of Theorem 1.

A.2.2 Theorem 2

Suppose that \tilde{Y}_1 and \tilde{Y}_2 are polynomial-tailed distributions, The proof is very similar to the proof of Theorem 1. Hence, we only provide high-level explanation.

Part(a): Similar to the Theorem 1, now we use polynomial type tail bound to compute $n_f(\delta, p^\eta)$, we obtain

$$n > \min \left\{ -M + \sqrt{M^2 + (6d\kappa_\Gamma)^{-1}}, -M + \sqrt{M^2 + \frac{\alpha}{24d(\kappa_\Gamma + dM^2\kappa_\Gamma^2)}}, \frac{\alpha M}{16} \right\}^{-2} p\tilde{C}_P^2 \left(p^{\eta/m} \right)$$

where $\tilde{C}_P = \max(\|M_{X_1}^{-1}\|_\infty^2, \|M_{X_2}^{-1}\|_\infty^2) \{2m[m * (\max(K_{1m}, K_{2m}) + 1)]^{\frac{1}{2m}} (\max(\max_i((\Theta^*_{1^{-1}})_{ii}), \max_i((\Theta^*_{2^{-1}})_{ii})))\}^{\frac{1}{2}}$.

Part(b): Similary to the proof of theorem 1, based on the definition 1. we obtain $\tilde{\delta}_{f_i}$ for polynomial type tail,

$$\tilde{\delta}_{f_1} \leq \max(\|M_{X_1}^{-1}\|_\infty^2, \|M_{X_2}^{-1}\|_\infty^2) \{2m[m * (K_{1m} + 1)]^{\frac{1}{2m}} (\max_i((\Theta^*_{1^{-1}})_{ii}))^{\frac{1}{2}} p^{\frac{1}{2}} \left\{ \frac{p^{\eta/m}}{n} \right\}^{\frac{1}{2}} \},$$

$$\tilde{\delta}_{f_2} \leq \max(\|M_{X_1}^{-1}\|_\infty^2, \|M_{X_2}^{-1}\|_\infty^2) \{2m[m * (K_{2m} + 1)]^{\frac{1}{2m}} (\max_i((\Theta^*_{2^{-1}})_{ii}))^{\frac{1}{2}} p^{\frac{1}{2}} \left\{ \frac{p^{\eta/m}}{n} \right\}^{\frac{1}{2}} \}.$$

The main result in Theorem 1 can now be proved by substituting the above inequalities into the right-hand side of equation 24 with some algebra manipulation

$$\begin{aligned} \|\hat{\Delta} - \Delta^*\|_\infty &\leq \left[\kappa_\Gamma + 3d\kappa_\Gamma^2 M^2 \left(\frac{\alpha^2}{256} + \frac{\alpha}{8} \right) \right] \left[2\tilde{C}_P + \max \left\{ \frac{8\tilde{C}_P}{\alpha}, \left(\frac{6}{16} + \frac{32}{\alpha} \right) dM^2(\kappa_\Gamma + dM^2\kappa_\Gamma^2) \right\} \right] \\ &\quad + \left[\frac{6}{16} dM^2\kappa_\Gamma^2(\alpha + 32)\tilde{C}_P \right] \sqrt{p} \left[\frac{p^{\eta/m}}{n} \right]^{\frac{1}{2}}. \end{aligned}$$

Similar to the previous proof, let \tilde{C}_{P_0} be defined as

$$\min \left\{ -M + \sqrt{M^2 + (6d\kappa_\Gamma)^{-1}}, -M + \sqrt{M^2 + \frac{\alpha}{24d(\kappa_\Gamma + dM^2\kappa_\Gamma^2)}}, \frac{\alpha M}{16} \right\}^{-2} \tilde{C}_P^2,$$

and \tilde{C}_{P_1} be defined as

$$\left[\kappa_\Gamma + 3d\kappa_\Gamma^2 M^2 \left(\frac{\alpha^2}{256} + \frac{\alpha}{8} \right) \right] \left[2\tilde{C}_P + \max \left\{ \frac{8\tilde{C}_P}{\alpha}, \left(\frac{6}{16} + \frac{32}{\alpha} \right) dM^2(\kappa_\Gamma + dM^2\kappa_\Gamma^2) \right\} \right] + \left[\frac{6}{16} dM^2\kappa_\Gamma^2(\alpha + 32)\tilde{C}_P \right].$$

This completes the proof of Theorem 2.

A.2.3 Proof of Corollary 1 and Corollary 2

Consider the following inequality:

$$\|\hat{\Delta} - \Delta^*\|_F^2 = \sum_{i,j} (\hat{\Delta}_{ij} - B_{ij}^*)^2 = \sum_i (\hat{\Delta}_{ii} - \Delta_{ii}^*)^2 + \sum_{i \neq j} (\hat{\Delta}_{ij} - \Delta_{ij}^*)^2 \quad (25)$$

$$\leq p \|\hat{\Delta} - \Delta^*\|_\infty^2 + s \|\hat{\Delta} - \Delta^*\|_\infty^2 \quad (26)$$

$$= (s + p) \|\hat{\Delta} - \Delta^*\|_\infty^2, \quad (27)$$

We now show the spectral norm.

$$\|\hat{\Delta} - \Delta^*\|_2 \leq d \|\hat{\Delta} - \Delta^*\|_\infty \quad (28)$$

and that

$$\|\hat{\Delta} - \Delta^*\|_2 \leq \|\hat{\Delta} - \Delta^*\|_F \leq \sqrt{s + p} \|\hat{\Delta} - \Delta^*\|_\infty. \quad (29)$$

We obtain

$$\|\hat{\Delta} - \Delta^*\|_2 \leq \min\{\sqrt{s + p}, d\} \|\hat{\Delta} - \Delta^*\|_\infty. \quad (30)$$